Biointerface Research in Applied Chemistry
Open-Access Journal (ISSN: 2069-5837)

Article
Volume 15, Issue 5, 2025, 68
https://doi.org/10.33263/BRIAC155.068

Green Synthesis of Selenium Nanoparticles from *Nephelium lappaceum* L. Seeds (NL-SeNPs) for Antioxidant and Photocatalytic Applications

Siti Raudhatul Kamali [1,*], Dinar Suksmayu Saputri [2,*], Chang-Nan Chen [3], Nurul Ismillayli [4], Saprini Hamdiani [4], Dhony Hermanto [4]

[1] Department of Environmental Science, University of Mataram, Mataram 83125, Indonesia; sitikamali@unram.ac.id;
[2] Research Center for Food Technology and Processing, National Research and Innovation Agency, Yogyakarta 55861, Indonesia; dina022@brin.go.id;
[3] Department of Applied Chemistry, Chaoyang University of Technology, Taichung 413310, Taiwan
[4] Department of Chemistry, University of Mataram, Mataram 83125, Indonesia
* Correspondence: sitikamali@unram.ac.id (S.R.K.); dina022@brin.go.id (D.S.S.);

Received: 12.05.2025; Accepted: 24.07.2025; Published: 10.08.2025

Abstract: Selenium nanoparticles (SeNPs) have acquired significant interest owing to their distinctive physicochemical characteristics and broad spectrum of application possibilities. In this study, SeNPs were synthesized using *Nephelium lappaceum* L. (NL) seed extract and assessed for both antioxidant and photocatalytic capabilities. The successful synthesis of NL-SeNPs was designated by a noticeable color shifting from yellow to red and validated by a UV–Vis absorbance peak at 263 nm. FTIR studies confirmed the existence of functional groups representative of various chemical compounds, including phenols and amines, which likely contributed to the reduction and stabilization of NL-SeNPs. The produced NL-SeNPs had a spherical morphology with an average particle size of approximately 100.94 nm and demonstrated notable colloidal stability, as indicated by a zeta potential of –30.7 mV. Their antioxidant activity showed moderate free radical scavenging efficiency in comparison to ascorbic acid, with maximum inhibition rates of 47.62% and 40.67% at a concentration of 70 µg/mL, and IC_{50} values of approximately 95.25 µg/mL and 112.44 µg/mL in the DPPH and ABTS assays, respectively. Furthermore, the photocatalytic performance of NL-SeNPs significantly enhanced the degradation of methylene blue, achieving approximately 69.40% removal after three hours under 365 nm UV irradiation. These findings show that NL-SeNPs work both as antioxidants and photocatalysts, making them useful for medical uses and eco-friendly cleaning or treatment processes.

Keywords: selenium nanoparticles; green synthesis; *Nephelium lappaceum* L. seed extract; antioxidant activity; photocatalytic degradation.

1. Introduction

Nanoparticles (NPs) are ultrafine particles, typically ranging from 1 to 100 nanometers in size, and exhibit diverse physicochemical properties that are highly dependent on their size and surface characteristics [1]. Recently, significant research has focused on metal nanoparticles (MNPs) such as silver (Ag), selenium (Se), copper (Cu), gold (Au), zinc (Zn), iron (Fe), and nickel (Ni), among others, due to their notable properties. These properties have

proven valuable in various applications such as catalysis, material composites, diagnostics and therapeutics, sensors, and optoelectronic technologies [2]. Selenium, a trace element and a key component of selenoproteins and selenocompounds, is crucial for the proper functioning of the immune response. It is essential for reproduction, DNA synthesis, thyroid hormone production, and the regulation of redox processes and iodine metabolism.

Additionally, selenium exhibits anti-inflammatory and antiviral properties, offering protection against infections and oxidative stress. Its high photoconductivity and low melting point make it highly effective in catalyzing organic hydration and oxidation reactions. Selenium deficiency can lead to severe health issues, including hepatic necrosis, muscle dystrophy, thyroid problems, and conditions impacting heart function, skeletal, and tissues [3,4]. Selenium is a vital component for all living creatures; nonetheless, its toxicity at elevated concentrations restricts its practical application. However, selenium nanoparticles exhibit reduced toxicity and diminished sub-chronic harmful effects compared to other selenium forms [5]. Selenium nanoparticles (SeNPs) are unique nanomaterials among other metallic nanoparticles, offering a diverse array of applications across various fields, including electronic devices, optical technology, catalytic processes, food packaging, medical practice, and biological sensors [2].

Selenium is essential for the activation of enzymes that protect the body and mitigate cellular damage induced by free radicals. Selenium nanoparticles (SeNPs) have shown superior efficacy compared to other forms of selenium in augmenting selenoprotein expression, neutralizing free radicals, and protecting DNA from oxidative stress. Consequently, SeNPs are widely explored for their antioxidant, antibacterial, and anticancer properties [1,4]. Nanomaterials are emerging as a viable alternative to antibiotics for the treatment of bacterial infections. Selenium, a vital nutrient with significant biological functions, is particularly appealing for integration with antibacterial agents. Selenium nanoparticles have demonstrated notable antimicrobial activity, particularly against *Aspergillus flavus*, *Bacillus subtilis*, *Candida albicans*, *Escherichia coli*, *Pseudomonas aeruginosa*, *Staphylococcus aureus*, tobacco meadow, and pitcher plant [1,6,7]. Notwithstanding the myriad benefits of selenium nanoparticles (SeNPs) compared to organic and inorganic selenium compounds, a major challenge remains their poor cellular uptake. To overcome this challenge, the biosynthesis of SeNPs is favored due to its potential to improve the biological compatibility and consistency [3].

Nanoparticles can be created via several processes, typically categorized into the chemical, physical, and biological approaches. However, chemical synthesis commonly employs toxic reducing and stabilizing agents, which may restrict their applicability in biological systems. Conversely, biological substances originating from extracts of plants and microorganisms are considered as superior alternatives, offering cost-effective, **e**nvironmentally friendly, and non-toxic approaches for nanoparticle production. Plant extracts, which serve as agents for reduction, transferring electrons to metal ions, facilitating the conversion into nanoparticles [3-5,8]. The biosynthesis of selenium nanoparticles (SeNPs) is a straightforward, one-step process that avoids the need for toxic chemicals, high temperatures, or complex equipment. Upon the addition of precursors to the bioextract, the solution typically changes color to red, red-orange, or orange, indicating the formation of selenium-containing compounds and the development of colloidal selenium nanoparticles (SeNPs). Following this, stabilization and capping of the nanoparticles occur naturally. Selenium compounds in their

elemental (Se^0) form are notably less toxic, enhancing their potential as therapeutic agents in combating various diseases [4].

Nephelium lappaceum L. is a significant tropical fruit extensively farmed in Southeast Asia, South America, Australia, and various African nations. South East Asian countries are among the foremost suppliers and manufacturers of this fruit. Between 2015 and 2017, Indonesia emerged as the top producer, with an average annual output of 692.0 thousand metric tons, accounting for 49.9% of the overall production. Thailand recorded 344.8 thousand metric tons (24.9%), Vietnam produced 261.4 thousand metric tons (18.8%), Malaysia with 62.7 thousand metric tons (4.5%), and the Philippines with 7.7 thousand metric tons (0.6%) [9,10]. The substantial production of *N. lappaceum* L. fruits generates large volumes of by-products. On a dry weight basis, the fruit consists of approximately 45.7% peel, 44.8% pulp, 9.5% seed, and 6.1% embryo. The seeds and peels, the primary leftovers of consumption or industrial processing, are frequently disposed of as waste items [10,11].

A promising strategy for valorizing *Nephelium lappaceum* L. waste or biomass is its utilization as a precursor in the green synthesis of nanoparticles. Selenium nanoparticles (SeNPs) synthesized from plant extracts are produced under mild, cost-effective conditions through a redox reaction facilitated by plant metabolites, which act as natural reducing, stabilizing, and capping agents. The extracts are abundant in bioactive chemicals, including phenols, terpenoids, and alkaloids, which exhibit inherent antibacterial properties that enhance the biological efficacy of the antimicrobial nanomaterials. Polyphenols contribute to nanoparticle formation through their functional groups. At the same time, flavonoids chelate metal ions via carbonyl groups or by donating electrons, playing a key role not only in reduction but also in the nucleation and aggregation processes. Stabilization is crucial to prevent agglomeration and regulate nanoparticle growth, typically achieved by coating the particles with a polymer or surfactant layer to minimize interparticle interactions. Plant-derived reducing agents act as electron donors, converting selenium ions into nanoparticles, while secondary metabolites further support the green synthesis of SeNPs by facilitating reduction, preventing agglomeration, and facilitating the development of smaller, more stable components [4,12,13]. The seeds of *Nephelium lappaceum* L. are rich in diverse phenolic compounds, including corilagin, geraniin, ellagic acid, monoterpene lactones (types 1 and 2), and kaempferol 3-O-β-D-glucopyranoside-7-O-α-L-rhamnopyranoside [9,14].

The use of *Nephelium lappaceum* (NL) peel extracts in the formation of nanoparticles, nanocrystals, and nanoplates has been reported in several studies [14-16]. While the use of NL seed extracts in nanoparticle production is still very limited. The current study aims to examine the possible impacts of NL seed extract in the synthesis of selenium nanoparticles (SeNPs) with photocatalytic and antioxidant properties.

2. Materials and Methods

2.1. Materials.

Sodium selenite (Na_2SeO_3) (≥98%) and 2,2-diphenyl-1-picrylhydrazyl (DPPH), 2,2-azinobis-(3-ethylbenzothiazoline-6-sulfonate) (ABTS) were acquired from Sigma-Aldrich, USA. Ascorbic acid, potassium persulfate, methylene blue, and methanol were all analytically graded and obtained from Merck, Germany.

2.2. Nephelium lappaceum L. seed extract preparation.

The preparation of the aqueous extract from *Nephelium lappaceum* L. seed was executed following the method outlined by Chankaew *et al*. [17] with a few adjustments. NL fruits were collected from West Lombok Island, Indonesia. Immediately after collection, the seeds were separated from the peels and pulp, then washed and dried at 75°C for 24 hours. After drying, the seeds were pulverized into a delicate dark brown powder employing a hammer mill. The obtained powder was preserved in dark containers at 4°C for subsequent use. Furthermore, 200 g of the dried seed powder was extracted with 100 mL of deionized water using an ultrasonicator for 15 minutes. The extract was then separated using Whatman No.1 filter paper and stored at 4°C for future analyses.

2.3. Synthesis of NL-SeNPs.

The NL-SeNPs were developed following a process described by Rao *et al*. [18] with minor alterations. In brief, 100 mL of aqueous NL seed extract was combined with 25 mL of 50 mM sodium selenite and maintained at room temperature for 12 hours with agitation at 50-100 rpm. The appearance of a brick-red hue in the product's reaction signified the successful formation of biogenic selenium nanoparticles (SeNPs). The SeNPs were isolated by centrifugation at 15,000 rpm, washed with distilled water to remove residual impurities, and subjected to a second round of centrifugation to ensure purification. The dried pellet was crushed using a mortar and pestle. The resultant brick-red powder was utilized for various characterizations.

2.4. Characterization of NL-SeNPs.

2.4.1. Ultraviolet visible (UV-Vis) spectroscopy.

The optical characteristics of NL-SeNPs were analyzed using UV–Visible spectrophotometry. The absorption spectra were acquired with a UV–Vis spectrophotometer (Lambda Perkin Elmer, Japan) throughout a wavelength range from 200 to 800 nm.

2.4.2. Fourier transform infrared (FTIR) spectroscopy.

The existence of diverse functional groups in the phytochemical compounds of NL seed extract was validated via Fourier Transform Infrared (FTIR) spectroscopy (Perkin Elmer, USA). FTIR spectroscopy of the NL-SeNPs solution was performed by recording spectra within the wavelength range of 4000–400 cm^{-1}.

2.4.3. Scanning electron microscopy (SEM).

The morphological characteristics of the synthesized NL-SeNPs were examined through Scanning Electron Microscopy (SEM SU3500, Japan). SEM images were captured at various magnifications to observe the surface morphology.

2.4.4. Transmission electron microscopy (TEM).

Transmission electron microscopy (TEM HT7700, Japan) was conducted to analyze the size distribution and precise morphology of the NL-SeNPs. Before imaging, the NL-SeNPs

were sonicated to ensure uniform dispersion and then carefully deposited onto a copper-coated grid for microscopic observation.

2.4.5. Energy dispersive X-ray (EDX).

EDX analysis was conducted to ascertain the constituent elements of the NL-SeNPs. The analysis provided semi-quantitative data, identifying the presence and relative abundance of elements such as selenium, carbon, oxygen, and other possible elements of NL-SeNPs.

2.4.6. X-ray diffraction (XRD).

The crystalline structure and phase composition of the synthesized NL-SeNPs were characterized by X-ray diffraction (XRD) using an XPert MPD diffractometer with Cu Kα radiation (λ = 1.5406 Å), operated at 40 kV and 30 mA.

2.4.7. Zeta potential.

The surface charge and colloidal stability of the synthesized NL-SeNPs were evaluated by the Nano Particle Analyzer (Horiba SZ-100, Japan). Prior to analysis, the nanoparticle suspension was diluted with deionized water to an appropriate concentration to avoid multiple scattering effects. Measurements were conducted at ambient temperature (25 ± 1°C) using a disposable capillary cell.

2.4.8. In vitro antioxidant assays.

2.4.8.1. DPPH (1,1 diphenyl 2-picryl hydrazyl) assay.

The scavenging activity of the synthesized NL-SeNPs was evaluated based on the DPPH test according to the technique of Sobuj *et al*. [19]. The antioxidant potential was assessed by evaluating the reduction of stable DPPH radicals to diphenyl picryl hydrazine, which is indicated by a visible color change from deep purple to yellow, and quantified spectrophotometrically at 517 nm. Various concentrations of NL-SeNPs (10–70 µg/mL) were added together with 3 mL of 0.1 mM DPPH solution and maintained in darkness for 30 minutes. Ascorbic acid functioned as a reference, while a DPPH solution devoid of the sample acted as the control, and the scavenging ability was determined using the equation:

$$\%\ inhibition = \frac{(Abs\ control - Abs\ sample)}{Abs\ control} \times 100\% \quad (1)$$

2.4.8.2. ABTS assay.

The synthesized NL-SeNPs were tested for their scavenging activity using ABTS (2,2'-Azino-bis (3-ethylbenzothiazoline-6-sulfonic acid), in accordance with the methods reported by Sobuj *et al*. [19] with small modifications. A practical solution was ready by combining 7 mM ABTS and 2.45 mM potassium persulfate in a 1:1 ratio with water. The percent inhibition of the ABTS radical by NL-SeNPs was according to their capacity to scavenge the cationic free radical. Various quantities of NL-SeNPs (10–70 µg/mL, 200 µL) were combined with 3800 µL of ABTS solution and kept in the dark for 14 hours. The intensity of color reduction was quantified at 734 nm. Ascorbic acid was used as a reference, while the ABTS solution in the

absence of the sample served as the control. The scavenging inhibition capacity percentage of ABTS+ for the extract was determined using the formula:

$$\%\ inhibition = \frac{(Abs\ control - Abs\ sample)}{Abs\ control} \times 100\% \quad (2)$$

2.4.9. Photocatalytic activity.

The examination of photocatalytic performance was conducted following the specified procedure outlined by Indhira *et al*. [20]. Specifically, 10 mg of SeNPs (used as a catalyst) was dispersed in 100 mL of methylene blue (MB) solution at a concentration of 50 mg/L and magnetically agitated for 30 minutes at neutral pH and room temperature to achieve an equilibrium condition of adsorption–desorption. The photocatalytic effectiveness of the SeNPs was then assessed under both dark conditions and UV irradiation at 365 nm for 3 hours. Changes in absorbance at 660 nm were observed at specified time intervals utilizing a UV–Vis spectrophotometer. The photocatalytic efficiency of the SeNPs was then calculated using the following equation:

$$Degradation\ rate\ (\%) = \frac{C_0 - C_i}{C_0}\ x\ 100\% \quad (3)$$

Where, C_0 is the initial concentration of the solution, C_i is the final concentration of MB solution

3. Results and Discussion

In this study, NL seed extract was used as the raw material for the green synthesis of NL-SeNPs. The extract is recognized for its abundance of diverse bioactive metabolites, including polyphenols, carbohydrates, anthocyanins, catechins, fats, and proteins [9,14,21]. The formation of NL-SeNPs mediated by the NL seed extract was visually verified through observable color changes in the reaction mixture. As illustrated in Figure 1, the successful synthesis was indicated by a distinct color transition upon mixing the NL seed extract with the sodium selenite solution. Initially, the NL seed extract appeared yellowish-white, which rapidly shifted to yellow upon the addition of sodium selenite. After 24 hours of continuous magnetic stirring under dark conditions, the solution turned red, and upon further reaction beyond 24 hours, it gradually became black. The transition in color to red visibly indicates the reduction of selenite to elemental selenium and the subsequent formation of selenium nanoparticles [22].

While the synthesis mechanism can vary depending on the specific plant part used, it is generally recognized that reducing agents commonly found in plant extracts—such as polyphenols, flavonoids, and terpenoids—play a key role in converting selenium ions into elemental selenium (Se^0). These compounds donate electrons that reduce selenium ions, facilitating the formation of selenium nanoparticles [23]. The observed reduction in activity is probably attributable to the presence of chemical components, including phenols and flavonoids, in the NL seed extract. NL seed extract contains phenolic compounds, flavonoids, and saponins, with a reported phenolic content of 39.55 mg of gallic acid per 100 g [24,25].

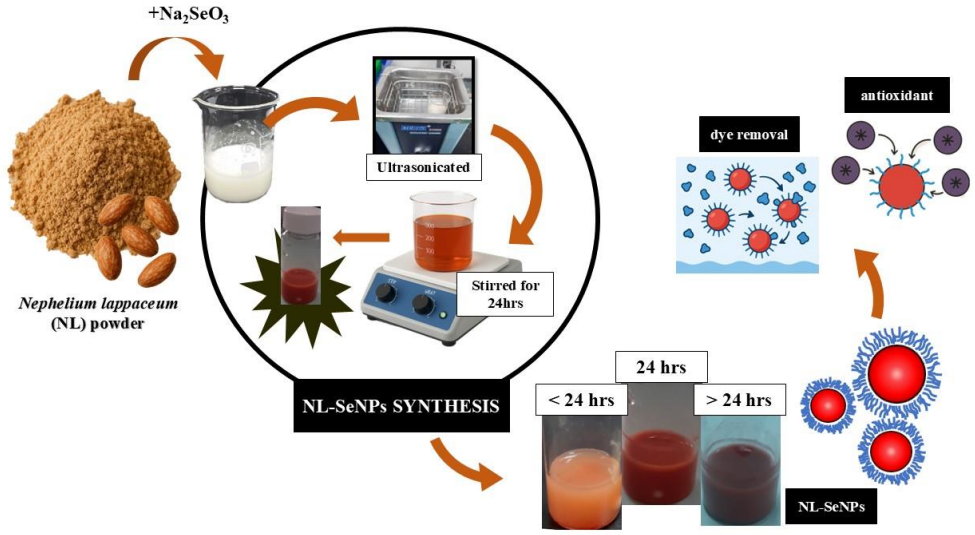

Figure 1. Synthesis and applications of NL-SeNPs in current research.

The green synthesis of nanoparticles involves polyphenols and other biomolecules acting as ligands that form stable metal complexes. Upon heating, these complexes decompose to release nanoparticles. Hydroxyl groups, especially in ortho or para positions, bind metal ions and undergo oxidation to carbonyls, contributing to nanoparticle stabilization [26]. The choice of solvent and the biochemical constituents in the various extracts play a crucial role in the successful reduction of SeO_2^- to elemental selenium (Se^0) [27].

3.1. Characterization of NL-SeNPs.

3.1.1. Ultraviolet-visible analysis.

UV–Vis spectroscopy is a widely used technique for estimating the optical properties of nanoparticles, providing valuable information on their size, shape, and composition. The presence of Se-NPs has been verified by the appearance of distinctive absorption peaks within the UV range of 200–400 nm [28]. The UV–Visible absorption spectrum of the synthesized NL-SeNPs displayed a characteristic peak at 265 nm (Figure 2). This observation is consistent with previous research conducted by Shahabadi *et al*. [29], who documented that selenium nanoparticles synthesized using ascorbic acid and sodium selenate exhibited a maximum absorption at the same wavelength. Moreover, SeNPs synthesized by Vasanthakumar *et al.* [22] using *Nannochloropsis oceanica* also showed a UV characteristic peak at 260 nm.

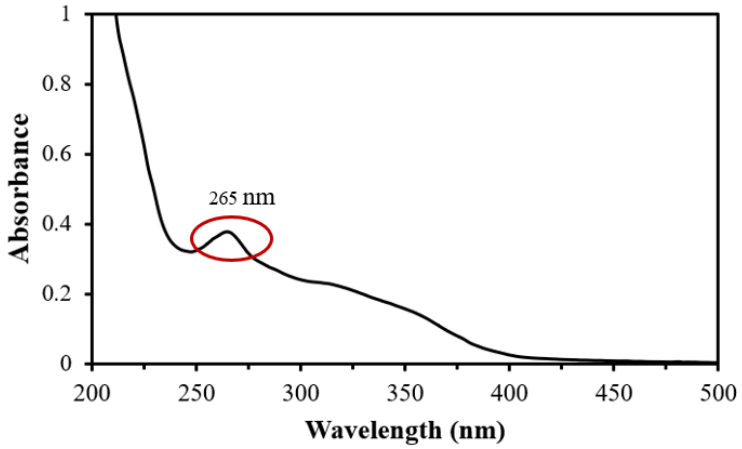

Figure 2. UV-Vis absorption spectra of NL-SeNPs.

The synthesized NL-SeNPs displayed an optical absorption peak at 265 nm, which is presumably attributed to the π→π* transitions of C=C bonds in sp²-hybridized carbon structures and aromatic systems [30]. Similarly, selenium nanoparticles synthesized from cinnamon extract exhibited a characteristic UV–Vis absorption peak at 284 nm [31,32], while chemically synthesized SeNPs exhibited a UV–Vis absorption peak at 298 nm [33]. In the present study, the formation of NL-SeNPs from NL seed extract was confirmed by a maximum absorbance peak, indicating successful nanoparticle synthesis. Notably, while selenite alone does not exhibit absorption in the UV–visible range, the NL seed extract exhibits notable absorption in the UV region, suggesting the presence of polyphenolic compounds. These polyphenols, along with vitamins, proteins, esters, and flavonoids found in the extract, are rich in hydroxyl groups that contribute to their strong reducing capacity, enabling the reduction of selenium ions. Additionally, amino and carbonyl groups in biomacromolecules are believed to form strong complexes with selenium species, stabilizing the nanoparticles by capping and preventing their aggregation [34].

3.1.2. FTIR analysis.

FTIR spectroscopic analysis was conducted to validate the involvement of NL seed extract in the biosynthesis of NL-SeNPs. FTIR spectroscopy detects functional groups on the surface of nanoparticles by examining the vibrational frequencies of their chemical bonds. Figure 3 displays the FTIR spectra of both the aqueous seed extract of NL and the synthesized NL-SeNPs.

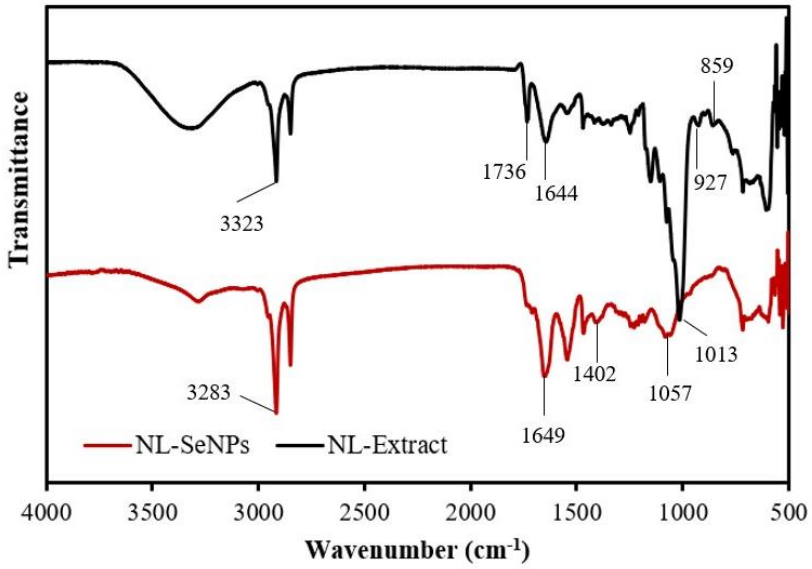

Figure 3. FTIR spectra of NL-SeNPs and NL-extract.

The FTIR profile of the aqueous NL seed extract indicated a prominent peak at 3323 cm^{-1}, corresponding to the–OH group and N-H bond in amide groups. During the NL-SeNPs biosynthesis, this peak shifted to 3283 cm^{-1}, indicating interaction between selenium and the hydroxyl group via hydrogen bonding, which facilitated NL-SeNPs synthesis [34,35]. Similarly, Anu *et al*. [36] synthesized SeNPs using garlic (Allium sativum) cloves extract and reported broad absorption peaks in the range of 3200–3400 cm^{-1}, which were attributed to the presence of hydroxyl (–OH) and amine (–NH) functional groups involved in the nanoparticle formation. Additional peaks observed in the aqueous extract included bands at 2917 cm^{-1} and 2851 cm^{-1} corresponding to aliphatic C–H stretching vibration; 1736 cm^{-1} (carboxylic acid O–

H stretch), 1644 cm^{-1} (amide I stretch–the characteristic region of proteins) [22], 1547 cm^{-1} (C=C aromatic stretch), and 1471 cm^{-1} (C–O stretch) [30,35]. Notably, the peak at 1736 cm^{-1} (carbonyl C=O stretch) disappeared in the NL-SeNPs, suggesting its role in nanoparticle formation [37,38].

Similarly, the peak at 1644 cm^{-1} (amide I stretch) shifted to 1649 cm^{-1}, indicating protein interaction with selenium via amine groups during the biosynthesis process. In a study by Ezhuthupurakkal *et al*. [39], the FTIR spectrum of Allium sativum-mediated SeNPs showed a shift in the peak from 1641.4 cm^{-1} to 1656 cm^{-1}, which may be attributed to modifications in pre-existing functional groups on the nanoparticle surface. These peaks were associated with the interaction between SeNP and protein in the solution [40]. Additionally, peaks at 1211 cm^{-1}, 1013 cm^{-1}, and 718 cm^{-1} observed in the FTIR spectrum of the aqueous seed extract are attributed to C–H bending in alkyl groups, C–N stretching in amines, and C–X stretching in alkyl halides, respectively [32]. A new peak observed at 1402 cm^{-1} in the NL-SeNPs corresponds to the C–N stretching vibration of aromatic amino group due to complexation with selenium ions [35]. In the aqueous NL seed extract, a strong absorption band at 1013 cm^{-1} was red-shifted to 1057 cm^{-1} in the NL-SeNPs, which is associated with Se–O stretching vibrations. This shift indicates the oxidation of proteins and polyphenols during the synthesis of selenium nanoparticles [37]. Multiple hydroxyl groups (-OH) found in constituents such as polyphenols exhibit strong reducing properties, enabling the conversion of selenite ions (Se4+) to elemental selenium atoms (Se0). Moreover, the presence of a carbonyl group, as revealed in the analysis, supports its role as a stabilizing agent. This stabilization is associated to the high surface energy of selenium atoms, which drives them to aggregate into nanoparticles to minimize surface energy. Stable SeNPs are formed when selenium atoms aggregate and establish complex interactions with bioactive macromolecules, thereby lowering surface energy and forming a protective coating around the nanoparticles [41]. El-Sayed *et al*. [35] reported that peaks at 1057 cm^{-1} (C–N), 1400 cm^{-1} (C–NH), and 1649 cm^{-1} (H–NH) are indicative of carbohydrate and protein characteristics, respectively. FTIR analysis confirmed the presence of functional groups on the nanoparticle surface, with proteins and carbohydrates being the predominant components on the NL-SeNPs. The identified functional groups arise from the conjugated biomolecules functioning as reducing and stabilizing agents on the surface of selenium nanoparticles [35]. The peaks at 927 cm^{-1} and 859 cm^{-1} observed in the NL seed extract disappeared in the NL-SeNPs, likely due to the oxidation of aldehyde functional groups [34]. The FTIR spectra thus verify the surface functionalization of NL-SeNPs by biomolecules involved in the synthesis process.

3.1.3. Scanning electron microscopy (SEM) and transmission electron microscopy (TEM) analysis.

The morphology and particle size of the produced NL-SeNPs were analyzed using SEM and TEM. Figures 4a and 4b revealed that the primary morphology of the selenium nanoparticles was spherical. Image analysis using ImageJ software indicated that the particle size varied from 70 to 130 nm, with an average diameter of approximately 100.94 nm (Figure 4c). These findings are consistent with previous reports, where spherical SeNPs synthesized using green tea and black tea extracts exhibited average sizes of 108 nm and 102 nm, respectively [42].

Plant extracts offer several advantages in nanoparticle synthesis, enabling the production of larger quantities with enhanced stability and diverse morphologies, such as cubic,

spherical, and irregular shapes. The specific extract or organism used influences nanoparticle size and shape, as variations in metabolite concentrations affect the synthesis process [26,43].

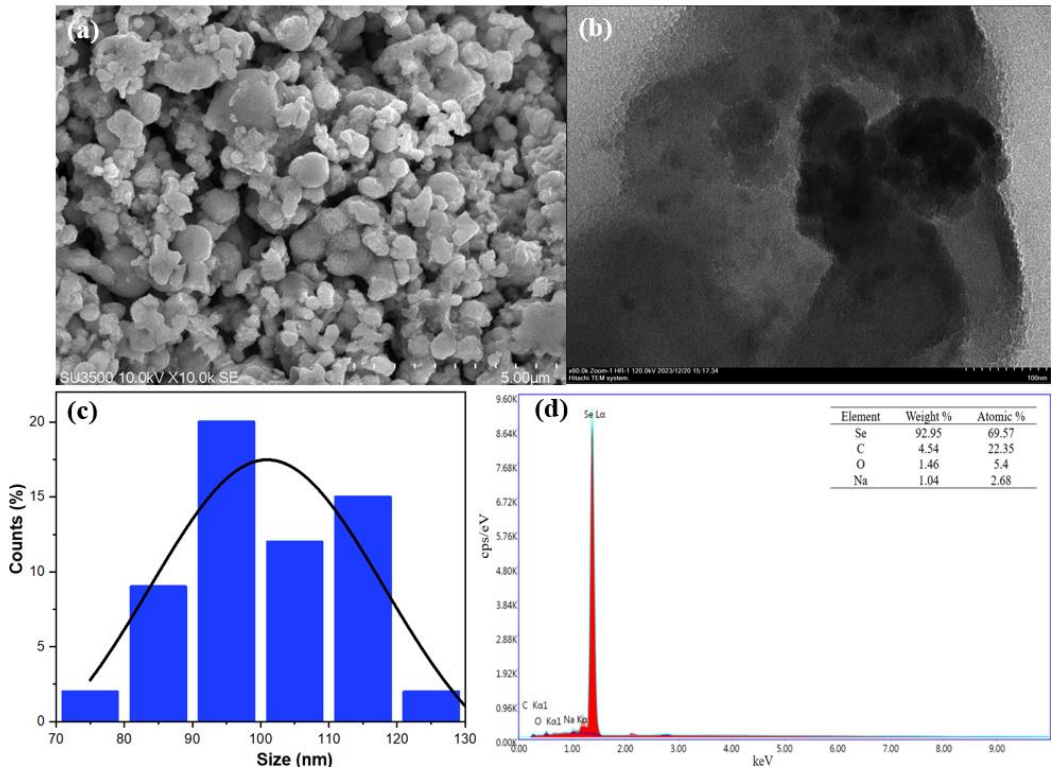

Figure 4. (a) SEM micrograph of NL-SeNPs (image at ×10000 magnification, scale bar = 5 µm); **(b)** TEM micrograph of NL-SeNPs (image at ×60000 magnification, scale bar = 100 nm); **(c)** Histogram of particle size distribution of NL-SeNPs; **(d)** EDX spectrum of NL-SeNPs.

The high abundance of selenium, measured at approximately 69.57%, confirms the successful synthesis of NL-SeNPs. In contrast, the existence of oxygen and carbon elements can be attributed to biomaterials functioning as capping agents on the nanoparticle surfaces. It is widely recognized that phytochemicals are typically associated with selenium nanoparticles synthesized from plant extracts [20]. Amino and carbonyl groups in the extracts are considered key bioactive components in nanoparticle encapsulation, as they lower surface free energy and improve particle stability [34]. Moreover, Gunti *et al* [37] highlighted that the presence of active biomolecules during synthesis notably affects the final size of the nanoparticles.

Meanwhile, the NL-SeNPs synthesized in this study demonstrated relatively small particle sizes, ranging from 70 to 130 nm, accompanied by some degree of aggregation. These results are consistent with previous studies, which reported *Moringa oleifera*-derived SeNPs with diameters below 100 nm—specifically, 10.47–28.5 nm from leaf extracts and 15.47–32.8 nm from bark extracts [41,44]. Similarly, SeNPs synthesized using *Tinospora cordifolia* stem extract and *Cassia javanica* flowers extract exhibited particle sizes ranging from 35 to 200 nm, with a mean diameter of 140.46 nm [32,45]. Similarly, studies using *Alangium salviifolium* leaf and fruit extract reported [46] predominantly spherical SeNPs with sizes ranging from 200 nm to 4 µm. Smaller particles (200–500 nm) reflected successful synthesis and stabilization, while larger ones suggested agglomeration or incomplete capping. Variations in size and shape were influenced by stabilizer properties, surface coating, and evaporation during preparation. In contrast, chemically synthesized SeNPs by Huong *et al.* [47] and Nagdalian *et al*. [48] typically range from 40 to 60 nm. It is noteworthy that smaller nanoparticles typically require a higher concentration of stabilizing biomolecules on their surfaces to maintain structural stability [49].

Furthermore, Gunti *et al*. [37] highlighted that nanoparticle size is significantly influenced by the specific nature and composition of the active compounds present in the biomaterials used during synthesis.

3.1.4. Energy dispersive X-ray (EDX) analysis.

Energy Dispersive X-ray Spectroscopy was employed to assess the elemental composition of the NL-SeNPs and to confirm the existence of selenium. Figure 4d displays the EDX spectrum along with the corresponding elemental weight percentages. The surface composition revealed prominent signals for selenium (69.57%), carbon (22.35%), oxygen (5.4%), and sodium (2.68%). The high intensity and proportion of selenium in the EDX spectrum confirmed the successful synthesis of selenium-rich nanoparticles with minimal contamination from other elements.

3.1.5. X-ray diffraction (XRD) analysis.

The X-ray diffraction pattern result reveals that NL-SeNPs are amorphous (Figure 5). A prominent diffraction peak occurs at an angle of 2θ of approximately 19°.

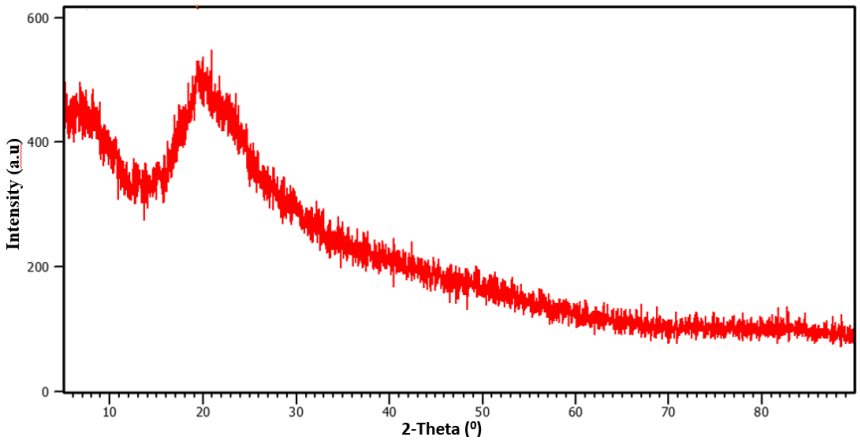

Figure 5. X-ray diffraction (XRD) pattern of the synthesized NL-SeNPs.

The XRD results obtained are consistent with previous findings, where nano-selenium exhibited a prominent diffraction peak around 2θ = 19°, along with weaker reflections near 23° and 25° [50]. The broad nature of these peaks suggests that the synthesized selenium nanoparticles possess a predominantly amorphous structure, characterized by poor crystallinity, and are very small in size. A dispersion peak in the 18° – 29° range was also observed in SeNPs synthesized from hawthorn [51] and *Curcuma longa* [52]. The detected structural amorphism is probably due to the many bioactive substances in the NL seed extract used in the synthesis. The extract contains a diverse array of biomolecules, including polyphenols, flavonoids, vitamins, and other macromolecules, which include carboxyl, hydroxyl, and various other chemical groups [33,34].

3.1.6. Zeta potential analysis.

Zeta potential indicates nanoparticle surface charge and dispersion stability. High positive or negative values prevent aggregation and enhance stability, while also influencing interactions with cell membranes and proteins [28]. The zeta potential of the NL-SeNPs was measured at –30.7 mV, indicating that the polydispersed nanoparticle suspension possesses improved colloidal stability (Figure 6). This result is lower than that of chemically synthesized

SeNPs, which showed a zeta potential of –51.2 mV [33] as well as SeNPs synthesized with the help of halophilic bacteria *Halomonas elongata* QW6 IBRC-M (–51.2 mV) and *Salinicoccus iranensis* IBRC-M (–60.6 mV) [55]. Nevertheless, NL-SeNPs exhibited a zeta potential value higher than those synthesized using *Pistacia vera* L. peel extract (–13.2 mV) [27], *Bacillus paranthracis* (–22.9 mV), and a combination of *Prunus persica* leaf extract with *Aloe vera* gel (0.2–28.4 mV) [56].

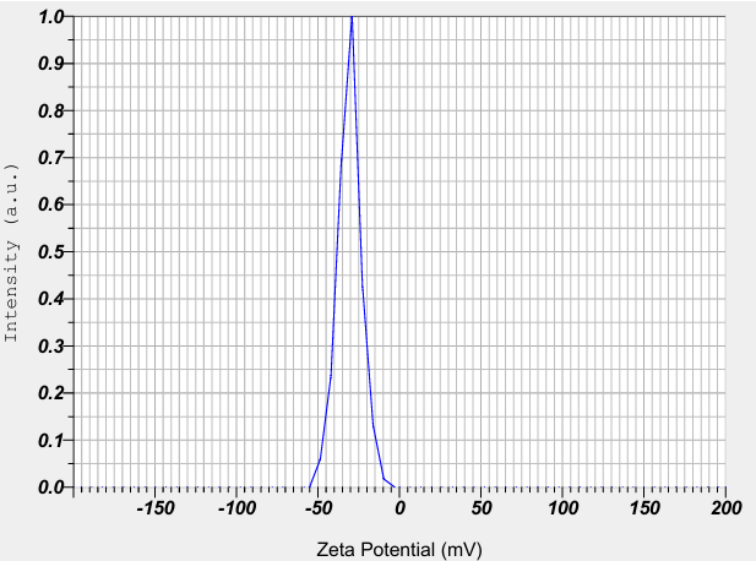

Figure 6. Zeta potential distribution of NL-SeNPs.

The negative zeta potential observed can be linked to the reducing agents involved in the oxidation of flavonoids and polyphenols in the NL seed extract, suggesting that repulsive electrostatic forces exist between the green-synthesized NL-SeNPs [32]. Absolute values of zeta potential of 30–40 mV indicate particularly good stability [57]. The negative zeta potential value of NL-SeNPs also indicates their excellent dispersibility and stability, with minimal aggregation [29]. A negative surface contributes to high physical stability by preventing destabilizing factors such as particle aggregation and fluctuation [27]. Stabilized particles do not convert into a black amorphous form, even after prolonged storage [55].

3.1.7. In-vitro antioxidant assays (DPPH and ABTS).

The antioxidant activity of the synthesized selenium nanoparticles (NL-SeNPs) was evaluated using the DPPH radical scavenging assay, which determines the capability of antioxidants to neutralize DPPH radicals. This reaction is evidenced by a distinct color shift from deep violet to yellow. As shown in Figure 7a, the radical scavenging activity of NL-SeNPs increased in a concentration-dependent manner, achieving a maximum inhibition of 47.62% at the highest tested concentration (70 µg/mL). In comparison, the standard antioxidant, ascorbic acid, exhibited significantly greater activity with an inhibition rate of 95.36% at the same concentration. The half-maximal inhibitory concentration (IC_{50}) values were calculated as 95.25 µg/mL for NL-SeNPs and 23.42 µg/mL for ascorbic acid (Figure 7b). These results indicate that while NL-SeNPs possess moderate antioxidant activity, their efficacy is notably lower than that of ascorbic acid.

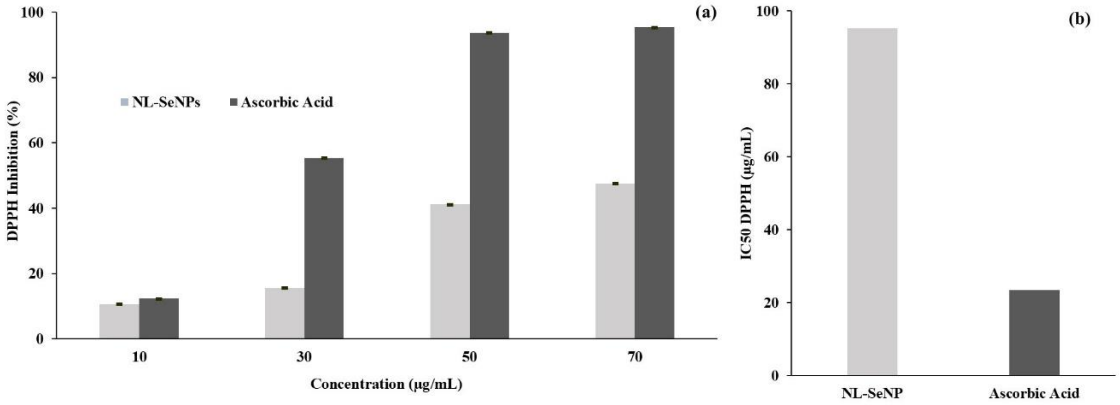

Figure 7. (a) DPPH radical scavenging activity; **(b)** IC_{50} of NL-SeNPs compared to ascorbic acid.

The ABTS (2,2′-azino-bis(3-ethylbenzothiazoline-6-sulfonic acid)) test was performed to assess the free radical scavenging capacity of NL-SeNPs. This approach relies on the reduction of the ABTS•$^{+}$ radical cation, leading to a reduction of the blue-green coloration. As shown in Figure 7b, NL-SeNPs demonstrated a concentration-dependent scavenging effect, reaching a maximum inhibition of 40.67% at 70 µg/mL. In contrast, ascorbic acid showed much stronger antioxidant activity, with a maximum inhibition of 91.33% at the same concentration (Figure 8a). The calculated IC_{50} values were 112.44 µg/mL for NL-SeNPs and 30.76 µg/mL for ascorbic acid (Figure 8b). These findings suggest that while NL-SeNPs exhibit antioxidant potential, their performance remains considerably lower than that of ascorbic acid, the standard reference antioxidant.

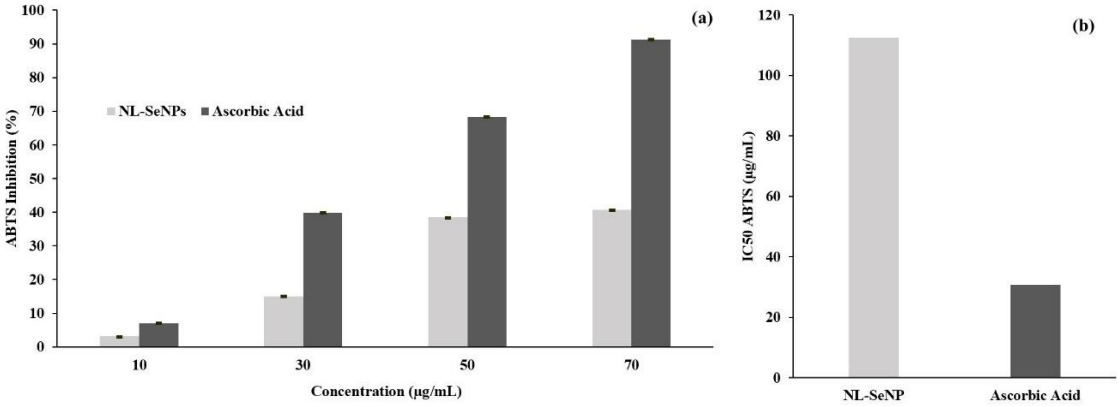

Figure 8. (a) ABTS radical scavenging activity; **(b)** IC_{50} of NL-SeNPs compared to ascorbic acid.

The antioxidant properties of the biosynthesized selenium nanoparticles (NL-SeNPs) were assessed through both DPPH and ABTS radical scavenging assays. The findings indicated that NL-SeNPs demonstrated moderate free radical neutralizing activity when benchmarked against the standard antioxidant, ascorbic acid. The DPPH assay is primarily responsive to lipophilic antioxidants and is particularly suitable for evaluating phenolic compounds and molecules with limited polarity. In contrast, the ABTS assay functions well in aqueous and hydrophilic systems and is capable of interacting with antioxidants that dissociate into anionic forms [58]. The higher IC_{50} value observed in the ABTS assay relative to DPPH suggests that NL-SeNPs might exhibit reduced efficiency in scavenging hydrophilic radicals, potentially due to the influence of hydrophobic phytochemicals derived from the plant extract used in the nanoparticle synthesis, which tend to perform better in less polar environments. Comparable trends have been reported in earlier studies, which synthesized selenium nanoparticles using an aqueous extract of *Annona muricata* fruit and found that DPPH radical scavenging activity

was higher than ABTS activity at equivalent concentrations, thereby aligning with the results of this study [18].

This result is lower than that of SeNPs synthesized from *Cassia javanica* flowers, which showed an IC_{50} of 53.34 µg/mL, and those synthesized using tea water extract, which exhibited antioxidant activity ranging from 99.1% to 99.9% [45,59]. However, the present study still demonstrates antioxidant activity comparable to that of SeNPs synthesized from hawthorn, which showed activity ranging from approximately 52–70% for DPPH and 42.71–65.53% for ABTS [51]. Similarly, SeNPs synthesized from *Moringa oleifera* polysaccharides exhibited ABTS antioxidant activity ranging from 32 – 81% [60]. Chemically synthesized SeNPs from bulk selenium powder and ethylenediamine also displayed antioxidant activity ranging from 20–59% for DPPH and 18–80% for ABTS [61].

The moderate antioxidant performance observed in both assays is consistent with prior findings by Puri and Patil [32], who reported that although biologically synthesized SeNPs do exhibit antioxidant activity, their radical scavenging capacity generally remains lower than that of well-established antioxidants such as ascorbic acid. Additionally, while some studies show that ABTS often detects higher antioxidant activity than DPPH in green-synthesized NL-SeNPs, this may be influenced by the selenium's electron-donating ability, nanoparticle morphology, synthesis conditions, and the nature of bioactive stabilizing agents or solvents used [37,38]. Nevertheless, the observable antioxidant capacity of NL-SeNPs suggests their potential application as complementary antioxidant agents in various fields.

3.1.8. Photocatalytic activity.

Selenium nanoparticles from NL seed extract (NL-SeNPs) were evaluated for their catalytic efficiency using methylene blue (MB) as an indicator dye. The breakdown of MB was monitored under both exposure to UV 365 nm and dark conditions. The findings highlighted that SeNPs showed a marked dependence on light for effective degradation (Figure 8). Under dark conditions, only 2.81% degradation was observed after 60 minutes, with a slight increase to 4.01% after 120 minutes. In contrast, when exposed to a 365 nm UV lamp, SeNPs significantly enhanced MB degradation, reaching 23.44% within the first hour and peaking at 69.40% after two hours (Figure 9). These findings are consistent with previous studies reporting that light exposure significantly enhances the photocatalytic performance of SeNPs, with MB degradation exceeding 60% under comparable conditions [20]. This comparison further supports the light-dependent photocatalytic nature of selenium-based nanomaterials.

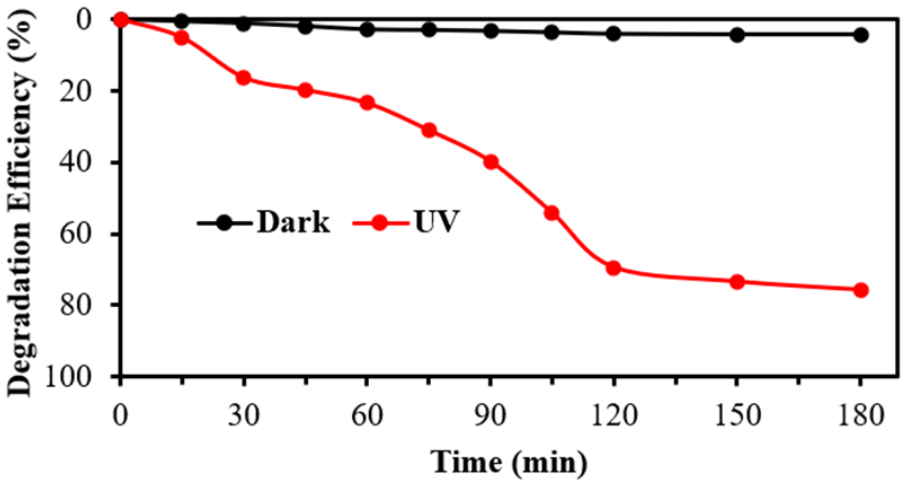

Figure 9. Photocatalytic removal of methylene blue (MB) by NL-SeNPs under UV and dark environments.

The photocatalytic efficiency of NL-SeNPs toward methylene blue (MB) dye is displayed in Figure 6. A progressive reduction in dye concentration was observed over the irradiation period, indicating the catalytic role of NL-SeNPs in facilitating MB degradation. Notably, the degradation efficiency under UV irradiation after 3 hours reached 69.40%, which was slightly higher than the 4.01% recorded under dark conditions, suggesting that light exposure enhances the photocatalytic activity.

The results reported here align with earlier studies by Menon *et al*. [63] and Indhira *et al.* [20], which emphasized that UV irradiation promotes more effective dye degradation, particularly due to the higher energy and reactivity associated with shorter wavelengths. A comparable trend was also documented by Hassanien *et al*. [64], who observed increased degradation efficiency under solar irradiation. The use of solar energy not only supports efficient photocatalysis but also offers operational safety and sustainability under ambient conditions.

Drawing upon both experimental evidence and prior literature, a degradation mechanism for MB in the presence of NL-SeNPs has been proposed and is illustrated in the following equation [65].

$$SeNPs \xrightarrow{hv} (h^+)_{(VB)} + (e^-)_{CB} \quad (4)$$

$$H_2O + (h^+)_{(VB)} \rightarrow H^+ + \cdot OH \quad (5)$$

$$O_2 + (e^-)_{CB} \rightarrow O_2^{\cdot -} \quad (6)$$

$$MB\ dye + \cdot OH + O_2^{\cdot -} \rightarrow organic\ ions\ CO_2 + H_2O \quad (7)$$

When exposed to light, NL-SeNPs function as photoactive centers by generating electron-hole pairs. Photoexcitation causes electrons to transition from the valence band (VB) to the conduction band (CB), leaving behind positively charged holes in the VB. These holes interact with water molecules to form hydroxyl radicals (•OH), while the electrons in the CB reduce oxygen molecules to produce superoxide radicals (O_2^{-}•). Both reactive oxygen species possess strong oxidative capabilities and play a crucial role in breaking down organic dyes such as methylene blue [20,40,41].

4. Conclusions

In conclusion, this study successfully demonstrated the green synthesis of selenium nanoparticles (NL-SeNPs) using *Nephelium lappaceum* L. seed extract, underscoring an environmentally sustainable approach to nanoparticle fabrication. The resulting NL-SeNPs exhibited spherical shape (~100.94 nm) and good stability (–30.7 mV zeta potential). They showed moderate antioxidant activity with IC_{50} values of 95.25 µg/mL (DPPH) and 112.44 µg/mL (ABTS), and achieved 69.40% degradation of methylene blue under UV light in two hours. Compared to previous reports, these results reinforce the feasibility of using plant-based nanomaterials. Future studies should focus on optimizing synthesis parameters, exploring biocompatibility, and testing their performance in real-world biological and environmental systems to enhance their functional efficacy through surface modification or integration into composite systems.

Author Contributions

Conceptualization, S.R.K. and D.S.S.; methodology, S.R.K.; validation, S.R.K., D.S.S., and N.I.; formal analysis, S.R.K.; investigation, S.H. and D.H.; resources, all authors; data curation,

all authors; writing—original draft preparation, S.R.K., C.N.C., and D.S.S.; writing—review and editing, S.R.K., C.N.C., and D.S.S.; visualization, D.S.S.; supervision, C.N.C.; funding acquisition, S.R.K., C.N.C., and D.S.S. All authors have read and agreed to the published version of the manuscript.

Institutional Review Board Statement

Not applicable.

Informed Consent Statement

Not applicable.

Data Availability Statement

Data supporting the findings of this study are available upon reasonable request from the corresponding author.

Funding

This research received no external funding.

Acknowledgments

The authors sincerely thank the University of Mataram for invaluable support during the research.

Conflicts of Interest

The authors declare no conflict of interest.

Abbreviations

Abbreviation	Definition
SeNPs	Selenium Nanoparticles
NL-SeNPs	*Nephelium lappaceum* L. Seed- Selenium Nanoparticles
NL	*Nephelium lappaceum* L.
UV-Vis	Ultraviolet visible
FTIR	Fourier Transform Infrared
DPPH	1,1 diphenyl 2-picryl hydrazyl
ABTS	2,2'-Azino-bis(3-ethylbenzothiazoline-6-sulfonic acid
NPs	Nanoparticles
MNPs	Metallic Nanoparticles
DNA	Deoxyribonucleic Acid
SEM	Scanning Electron Microscope
EDX	Energy Dispersive X-ray
XRD	X-ray Diffraction
MB	Methylene Blue
MO-SeNPs	Moringa Oleifera-Selenium Nanoparticles
TC-SeNPs	Tinospora Cordifolia-Selenium Nanoparticles
VB	Valence Band
CB	Conduction Band

References

1. Xiao, X.; Deng, H.; Lin, X.; Ali, A.S.M.; Viscardi, A.; Guo, Z.; Qiao, L.; He, Y.; Han, J. Selenium Nanoparticles: Properties, Preparation Methods, and Therapeutic Applications. *Chem. Biol. Interact.* **2023**, *378*, 110483, https://doi.org/10.1016/j.cbi.2023.110483.
2. Hussain, A.; Lakhan, M.N.; Hanan, A.; Soomro, I.A.; Ahmed, M.; Bibi, F.; Zehra, I. Recent Progress on Green Synthesis of Selenium Nanoparticles – a Review. *Mater. Today. Sustain.* **2023**, *23*, 100420, https://doi.org/10.1016/j.mtsust.2023.100420.
3. Bisht, N.; Phalswal, P.; Khanna, P.K. Selenium Nanoparticles: A Review on Synthesis and Biomedical Applications. *Mater. Adv.* **2022**, *3*, 1415–1431, https://doi.org/10.1039/D1MA00639H.
4. Mikhailova, E.O. Selenium Nanoparticles: Green Synthesis and Biomedical Application. *Molecules* **2023**, *28*, 8125, https://doi.org/10.3390/molecules28248125.
5. Sampath, S.; Sunderam, V.; Manjusha, M.; Dlamini, Z.; Lawrance, A.V. Selenium Nanoparticles: A Comprehensive Examination of Synthesis Techniques and Their Diverse Applications in Medical Research and Toxicology Studies. *Molecules* **2024**, *29*, 801, https://doi.org/10.3390/molecules29040801.
6. Khudier, M.A.A.; Hammadi, H.A.; Atyia, H.T.; Al-Karagoly, H.; Albukhaty, S.; Sulaiman, G.M.; Dewir, Y.H.; Mahood, H.B. Antibacterial Activity of Green Synthesized Selenium Nanoparticles Using *Vaccinium Arctostaphylos* (L.) Fruit Extract. *Cogent Food Agric.* **2023**, *9*, 2245612, https://doi.org/10.1080/23311932.2023.2245612.
7. Vahdati, M.; Tohidi Moghadam, T. Synthesis and Characterization of Selenium Nanoparticles-Lysozyme Nanohybrid System with Synergistic Antibacterial Properties. *Sci. Rep.* **2020**, *10*, 510, https://doi.org/10.1038/s41598-019-57333-7.
8. Ceylan, R.; Demirbas, A.; Ocsoy, I.; Aktumsek, A. Green Synthesis of Silver Nanoparticles Using Aqueous Extracts of Three Sideritis Species from Turkey and Evaluations Bioactivity Potentials. *Sustain. Chem. Pharm.* **2021**, *21*, 100426, https://doi.org/10.1016/j.scp.2021.100426.
9. Jahurul, M.; Azzatul, F.; Sharifudin, M.; Norliza, M.; Hasmadi, M.; Lee, J.; Patricia, M.; Jinap, S.; George, M.R.; Khan, M.F. Functional and nutritional properties of rambutan (Nephelium lappaceum L.) seed and its industrial application: A review. *Trends Food Sci. Technol.* **2020**, *99*, 367-374, https://doi.org/10.1016/j.tifs.2020.03.016.
10. Rakariyatham, K.; Zhou, D.; Rakariyatham, N.; Shahidi, F. Sapindaceae (Dimocarpus Longan and Nephelium Lappaceum) Seed and Peel by-Products: Potential Sources for Phenolic Compounds and Use as Functional Ingredients in Food and Health Applications. *J. Funct. Foods* **2020**, *67*, 103846, https://doi.org/10.1016/j.jff.2020.103846.
11. Tingting, Z.; Xiuli, Z.; Kun, W.; Liping, S.; Yongliang, Z. A Review: Extraction, Phytochemicals, and Biological Activities of Rambutan (Nephelium Lappaceum L) Peel Extract. *Heliyon* **2022**, *8*, e11314, https://doi.org/10.1016/j.heliyon.2022.e11314.
12. Ao, B.; Du, Q.; Liu, D.; Shi, X.; Tu, J.; Xia, X. A Review on Synthesis and Antibacterial Potential of Bio-Selenium Nanoparticles in the Food Industry. *Front. Microbiol.* **2023**, *14*, 1229838, https://doi.org/10.3389/fmicb.2023.1229838.
13. Aswathi, V.P.; Meera, S.; Maria, C.G.A.; Nidhin, M. Green Synthesis of Nanoparticles from Biodegradable Waste Extracts and Their Applications: A Critical Review. *Nanotechnol. Environ. Eng.* **2023**, *8*, 377–397, https://doi.org/10.1007/s41204-022-00276-8.
14. Kumar, B.; Smita, K.; Cumbal, L.; Angulo, Y. Fabrication of Silver Nanoplates Using Nephelium Lappaceum (Rambutan) Peel: A Sustainable Approach. *J. Mol. Liq.* **2015**, *211*, 476–480, https://doi.org/10.1016/j.molliq.2015.07.067.
15. Karnan, T.; Selvakumar, S.A.S. Biosynthesis of ZnO Nanoparticles Using Rambutan (Nephelium lappaceumL.) Peel Extract and Their Photocatalytic Activity on Methyl Orange Dye. *J. Mol. Struct.* **2016**, *1125*, 358–365, https://doi.org/10.1016/j.molstruc.2016.07.029.
16. Yuvakkumar, R.; Suresh, J.; Nathanael, A.J.; Sundrarajan, M.; Hong, S.I. Novel Green Synthetic Strategy to Prepare ZnO Nanocrystals Using Rambutan (Nephelium Lappaceum L.) Peel Extract and Its Antibacterial Applications. *Mater. Sci. Eng. C* **2014**, *41*, 17–27, https://doi.org/10.1016/j.msec.2014.04.025.
17. Chankaew, C.; Tapala, W.; Grudpan, K.; Rujiwatra, A. Microwave Synthesis of ZnO Nanoparticles Using Longan Seeds Biowaste and Their Efficiencies in Photocatalytic Decolorization of Organic Dyes. *Environ. Sci. Pollut. Res.* **2019**, *26*, 17548–17554, https://doi.org/10.1007/s11356-019-05099-w.

18. Rao, C.K.; Rosaiah, G.; Mangamuri, U.K.; Sikharam, A.S.; Kalagatur, N.K.; Kadirvelu, K. Biosynthesis of Selenium Nanoparticles from Annona Muricata Fruit Aqueous Extract and Investigation of Their Antioxidant and Antimicrobial Potentials. *Curr. Trends Biotechnol. Pharm.* **2022**, *16*, 101–107, https://doi.org/10.5530/ctbp.2022.1.10.
19. Sobuj, M.K.A.; Shemul, M.S.; Islam, Md.S.; Islam, Md.A.; Mely, S.S.; Ayon, M.H.; Pranto, S.M.; Alam, M.S.; Bhuiyan, M.S.; Rafiquzzaman, S.M. Qualitative and Quantitative Phytochemical Analysis of Brown Seaweed Sargassum Polycystum Collected from Bangladesh with Its Antioxidant Activity Determination. *Food Chem. Adv.* **2024**, *4*, 100565, https://doi.org/10.1016/j.focha.2023.100565.
20. Indhira, D.; Aruna, A.; Manikandan, K.; Albeshr, M.F.; Alrefaei, A.F.; Vinayagam, R.; Kathirvel, A.; Priyan, S.R.; Kumar, G.S.; Srinivasan, R. Antimicrobial and Photocatalytic Activities of Selenium Nanoparticles Synthesized from Elaeagnus Indica Leaf Extract. *Processes* **2023**, *11*, 1107, https://doi.org/10.3390/pr11041107.
21. Sirait, S.M.; Harpil, A.N.; Alma, D.T.; Andika, D.; Shakti, F.F.; Solihin, M.A.A.; Putra, S.M.S. Pemanfaatan Biji Rambutan (Nephelium lappaceum) sebagai Produk Pangan Inovasi Martabak Tepung Biji Rambutan. *WARTA AKAB* **2023**, *47*, 1-7, https://doi.org/10.55075/wa.v47i1.175.
22. Vasanthakumar, S.; Manikandan, M.; Arumugam, M. Green Synthesis, Characterization and Functional Validation of Bio-Transformed Selenium Nanoparticles. *Biochem. Biophys. Rep.* **2024**, *39*, 101760, https://doi.org/10.1016/j.bbrep.2024.101760.
23. Y. Alqaraleh, S.; Al-Zereini, W.A.; R. Mwafi, N.; M. Jaffal, S.; Al-Qtaitat, A.I. The Green Synthesis of Selenium Nanoparticles: A Comprehensive Review on Methodology, Characterization and Biomedical Applications. *Res. J. Pharm. Technol.* **2024**, 4054–4062, https://doi.org/10.52711/0974-360X.2024.00629.
24. Afzaal, M.; Saeed, F.; Bibi, M.; Ejaz, A.; Shah, Y.A.; Faisal, Z.; Ateeq, H.; Akram, N.; Asghar, A.; Shah, M.A. Nutritional, Pharmaceutical, and Functional Aspects of Rambutan in Industrial Perspective: An Updated Review. *Food Sci. Nutr.* **2023**, *11*, 3675–3685, https://doi.org/10.1002/fsn3.3379.
25. Mukaromah, A.H.; Cahyaningrum, D.G.; Putri, D.R.; Jannah, E.M.; Rinaldi, M.R.; Wardoyo, F.A.; Ariyadi, T.; Hikmah, A.N.; Darmawati, S. Antibacteria Activity Peel and Seed Extracts of Rambutan (Nephelium Lappaceum L.) Against MDR Bacteria Causing Urinary Tract Infections. *J. Biol. Biol. Edu.* **2023**, *15*, 432–440, https://doi.org/10.15294/biosaintifika.v15i3.39568.
26. Álvarez-Chimal, R.; Arenas-Alatorre, J.Á. Green Synthesis of Nanoparticles: A Biological Approach. In Advances in Green Chemistry - Prevention-Assurance-Sustainability (P-A-S) Approach, Shah, K.J., Ed.; IntechOpen: Rijeka, **2023**; https://doi.org/10.5772/intechopen.1002203.
27. Baran, M.F.; Keskin, C.; Baran, A.; Kurt, K.; İpek, P.; Eftekhari, A.; Khalilov, R.; Fridunbayov, I.; Cho, W.C. Green Synthesis and Characterization of Selenium Nanoparticles (Se NPs) from the Skin (Testa) of Pistacia Vera L. (Siirt Pistachio) and Investigation of Antimicrobial and Anticancer Potentials. *Biomass Conv. Bioref.* **2024**, *14*, 23623–23633, https://doi.org/10.1007/s13399-023-04366-8.
28. Ibrahim, S.S.S.; Ansari, Y.N.; Puri, A.V.; Patil, V.V.; Gaikwad, S.S.; Haroon, R.A. Recent Progress in the Green Synthesis, Characterization, and Applications of Selenium Nanoparticles. *BIO Integr.* **2024**, *5*, 969, https://doi.org/10.15212/bioi-2024-0063.
29. Shahabadi, N.; Zendehcheshm, S.; Khademi, F. Selenium Nanoparticles: Synthesis, in-Vitro Cytotoxicity, Antioxidant Activity and Interaction Studies with Ct-DNA and HSA, HHb and Cyt c Serum Proteins. *Biotechnol. Rep.* **2021**, *30*, e00615, https://doi.org/10.1016/j.btre.2021.e00615.
30. Nizam, N.U.M.; Hanafiah, M.M.; Mahmoudi, E.; Mohammad, A.W. Synthesis of Highly Fluorescent Carbon Quantum Dots from Rubber Seed Shells for the Adsorption and Photocatalytic Degradation of Dyes. *Sci. Rep.* **2023**, *13*, 12777, https://doi.org/10.1038/s41598-023-40069-w.
31. Behera, A.; Devi, Y.; Ryntathiang, L.; Jothinathan, M.K.D. Green Synthesis of Selenium Nanoparticles Using Cinnamomum Verum Extract and Their Antibacterial, Antioxidant, and Brine Shrimp Toxicity Effects. *Tex. Int. J. Public Health* **2024**, *12*, 1–13, https://doi.org/10.21522/TIJPH.2013.12.03.Art039.
32. Puri, A.; Patil, S. Tinospora Cordifolia Stem Extract-Mediated Green Synthesis of Selenium Nanoparticles and Its Biological Applications. *Pharmacogn. Res.* **2022**, *14*, 289–296, http://dx.doi.org/10.5530/pres.14.3.42.
33. Habeeb, Z.A.; Jameel, S.K.; Ahmed, M.E. Synthesis, Characterization, and Cytotoxic Evaluation of Selenium Nanoparticles. *Biomed. Pharmacol. J.* **2025**, *18*, 909–919, https://doi.org/10.13005/bpj/3139.
34. Wen, S.; Hui, Y.; Chuang, W. Biosynthesis and Antioxidation of Nano-Selenium Using Lemon Juice as a Reducing Agent. *Green Process. Synth.* **2021**, *10*, 178–188, https://doi.org/10.1515/gps-2021-0018.

35. EL-Sayed, A.I.M.; El-Sheekh, M.M.; Abo-Neima, S.E. Mycosynthesis of Selenium Nanoparticles Using Penicillium Tardochrysogenum as a Therapeutic Agent and Their Combination with Infrared Irradiation against Ehrlich Carcinoma. *Sci. Rep.* **2024**, *14*, 2547, https://doi.org/10.1038/s41598-024-52982-9.
36. Anu, K.; Singaravelu, G.; Murugan, K.; Benelli, G. Green-Synthesis of Selenium Nanoparticles Using Garlic Cloves (Allium Sativum): Biophysical Characterization and Cytotoxicity on Vero Cells. *J. Clust. Sci.* **2017**, *28*, 551–563, https://doi.org/10.1007/s10876-016-1123-7.
37. Gunti, L.; Dass, R.S.; Kalagatur, N.K. Phytofabrication of Selenium Nanoparticles From Emblica Officinalis Fruit Extract and Exploring Its Biopotential Applications: Antioxidant, Antimicrobial, and Biocompatibility. *Front. Microbiol.* **2019**, *10*, 931, https://doi.org/10.3389/fmicb.2019.00931.
38. Abdelhamid, A.E.; Ahmed, E.H.; Awad, H.M.; Ayoub, M.M.H. Synthesis and Cytotoxic Activities of Selenium Nanoparticles Incorporated Nano-Chitosan. *Polym. Bull.* **2024**, *81*, 1421–1437, https://doi.org/10.1007/s00289-023-04768-8.
39. Ezhuthupurakkal, P.B.; Polaki, L.R.; Suyavaran, A.; Subastri, A.; Sujatha, V.; Thirunavukkarasu, C. Selenium Nanoparticles Synthesized in Aqueous Extract of Allium Sativum Perturbs the Structural Integrity of Calf Thymus DNA through Intercalation and Groove Binding. *Mater. Sci. Eng. C* **2017**, *74*, 597–608, https://doi.org/10.1016/j.msec.2017.02.003.
40. Li, S.; Shen, Y.; Xie, A.; Yu, X.; Zhang, X.; Yang, L.; Li, C. Rapid, Room-Temperature Synthesis of Amorphous Selenium/Protein Composites Using*Capsicum Annuum L*Extract. *Nanotechnology* **2007**, *18*, 405101, https://doi.org/10.1088/0957-4484/18/40/405101.
41. Ahamad Tarmizi, A.A.; Nik Ramli, N.N.; Adam, S.H.; Abdul Mutalib, M.; Mokhtar, M.H.; Tang, S.G.H. Phytofabrication of Selenium Nanoparticles with Moringa Oleifera (MO-SeNPs) and Exploring Its Antioxidant and Antidiabetic Potential. *Molecules* **2023**, *28*, 5322, https://doi.org/10.3390/molecules28145322.
42. Al Jahdaly, B.A.; Al-Radadi, N.S.; Eldin, G.M.G.; Almahri, A.; Ahmed, M.K.; Shoueir, K.; Janowska, I. Selenium Nanoparticles Synthesized Using an Eco-Friendly Method: Dye Decolorization from Aqueous Solutions, Cell Viability, Antioxidant, and Antibacterial Effectiveness. *J. Mater. Res. Technol.* **2021**, *11*, 85–97, https://doi.org/10.1016/j.jmrt.2020.12.098.
43. Osman, A.I.; Zhang, Y.; Farghali, M.; Rashwan, A.K.; Eltaweil, A.S.; Abd El-Monaem, E.M.; Mohamed, I.M.; Badr, M.M.; Ihara, I.; Rooney, D.W. Synthesis of green nanoparticles for energy, biomedical, environmental, agricultural, and food applications: A review. *Environ. Chem. Lett.* **2024**, *22*, 841-887, https://doi.org/10.1007/s10311-023-01682-3.
44. Olaoye, A.B.; Owoeye, S.S.; Nwobegu, J.S. Facile Green Synthesis of Plant-Mediated Selenium Nanoparticles (SeNPs) Using Moringa Oleifera Leaf and Bark Extract for Targeting α-Amylase and α-Glucosidase Enzymes in Diabetes Management. *Hybrid Adv.* **2024**, *7*, 100281, https://doi.org/10.1016/j.hybadv.2024.100281.
45. Soliman, M.K.Y.; Amin, M.A.-A.; Nowwar, A.I.; Hendy, M.H.; Salem, S.S. Green Synthesis of Selenium Nanoparticles from Cassia Javanica Flowers Extract and Their Medical and Agricultural Applications. *Sci. Rep.* **2024**, *14*, 26775, https://doi.org/10.1038/s41598-024-77353-2.
46. Saravanan, K.; Madhaiyan, M.; Periyasamy, P.; Manivannan, P.; Bayrakdar, A.; Balakrishnan, V. Green Synthesis and Detailed Characterization of Selenium Nanoparticles Derived from Alangium Salviifolium (L.f) Wangerin. *Chem. Phys. Impact* **2025**, *10*, 100876, https://doi.org/10.1016/j.chphi.2025.100876.
47. Huong, N.T.; Tung, D.K.; Ky, V.H.; Nam, P.H.; Ngoc Anh, N.T. Synthesis of Nano-Selenium and Its Effects on Germination and Early Seedling Growth of Four Crop Plants. *AIP Adv.* **2024**, *14*, 025046, https://doi.org/10.1063/5.0188848.
48. Nagdalian, A.A.; Blinov, A.V.; Siddiqui, S.A.; Gvozdenko, A.A.; Golik, A.B.; Maglakelidze, D.G.; Rzhepakovsky, I.V.; Kukharuk, M.Y.; Piskov, S.I.; Rebezov, M.B. Effect of selenium nanoparticles on biological and morphofunctional parameters of barley seeds (Hordéum vulgáre L.). *Sci. Rep.* **2023**, *13*, 6453, https://doi.org/10.1038/s41598-023-33581-6.
49. Satgurunathan, T.; Bhavan, P.S.; Komathi, S. Green Synthesis of Selenium Nanoparticles from Sodium Selenite Using Garlic Extract and Its Enrichment on Artemia Nauplii to Feed the Freshwater Prawn Macrobrachium Rosenbergii Post-Larvae. *Res. J. Chem. Environ.* **2017**, *21*, 1–12.
50. Cavalu, S.; Prokisch, J.; Laslo, V.; Vicas, S. Preparation, Structural Characterisation and Release Study of Novel Hybrid Microspheres Entrapping Nanoselenium, Produced by Green Synthesis. *IET Nanobiotechnol.* **2017**, *11*, 426–432, https://doi.org/10.1049/iet-nbt.2016.0107.

51. Sun, J.; Li, J.; Yao, L.; You, F.; Yuan, J.; Wang, D.; Gu, S. Synthesis, Characterization and Antioxidant Activity of Selenium Nanoparticle Decorated with Polysaccharide from Hawthorn. *Food Measure* **2023**, *17*, 6125–6134, https://doi.org/10.1007/s11694-023-02124-y.
52. Mohamed Radzi, A.M.; Ahmad Tarmizi, Z.I.; Abdul Ghafar, N.A.A.; Mohd Talib, S.H.; Mohamed Isa, E.D. Green Synthesis of Selenium Nanoparticles and Its Electrochemical Properties. *E3S Web Conf.* **2024**, *516*, 02006, https://doi.org/10.1051/e3sconf/202451602006.
53. Jantapaso, H.; Mittraparp-arthorn, P. Phytochemical Composition and Bioactivities of Aqueous Extract of Rambutan (Nephelium Lappaceum L. Cv. Rong Rian) Peel. *Antioxidants* **2022**, *11*, 956, https://doi.org/10.3390/antiox11050956.
54. Hernández, C.; Ascacio-Valdés, J.; De La Garza, H.; Wong-Paz, J.; Aguilar, C.N.; Martínez-Ávila, G.C.; Castro-López, C.; Aguilera-Carbó, A. Polyphenolic Content, in Vitro Antioxidant Activity and Chemical Composition of Extract from Nephelium Lappaceum L. (Mexican Rambutan) Husk. *Asian Pac. J. Trop. Med.* **2017**, *10*, 1201–1205, https://doi.org/10.1016/j.apjtm.2017.10.030.
55. Tabibi, M.; Aghaei, S.; Amoozegar, M.A.; Nazari, R.; Zolfaghari, M.R. Characterization of Green Synthesized Selenium Nanoparticles (SeNPs) in Two Different Indigenous Halophilic Bacteria. *BMC Chem.* **2023**, *17*, 115, https://doi.org/10.1186/s13065-023-01034-w.
56. Shayan, S.; Hajihajikolai, D.; ghazale, F.; Gharahdaghigharahtappeh, F.; Faghih, A.; Ahmadi, O.; Behbudi, G. Optimization of Green Synthesis Formulation of Selenium Nanoparticles SeNPs) Using Peach Tree Leaf Extract and Investigating Its Properties and Stability. *Iran J. Biotechnol.* **2024**, *22*, https://doi.org/10.30498/ijb.2024.413943.3786.
57. Galić, E.; Radić, K.; Golub, N.; Vitali Čepo, D.; Kalčec, N.; Vrček, E.; Vinković, T. Utilization of Olive Pomace in Green Synthesis of Selenium Nanoparticles: Physico-Chemical Characterization, Bioaccessibility and Biocompatibility. *Int. J. Mol. Sci.* **2022**, *23*, 9128, https://doi.org/10.3390/ijms23169128.
58. Wołosiak, R.; Drużyńska, B.; Derewiaka, D.; Piecyk, M.; Majewska, E.; Ciecierska, M.; Worobiej, E.; Pakosz, P. Verification of the Conditions for Determination of Antioxidant Activity by ABTS and DPPH Assays—A Practical Approach. *Molecules* **2021**, *27*, 50, https://doi.org/10.3390/molecules27010050.
59. Sentkowska, A.; Pyrzyńska, K. Antioxidant Properties of Selenium Nanoparticles Synthesized Using Tea and Herb Water Extracts. *Appl. Sci.* **2023**, *13*, 1071, https://doi.org/10.3390/app13021071.
60. Tao, L.; Guan, C.; Wang, Z.; Wang, Y.; Gesang, Q.; Sheng, J.; Dai, J.; Tian, Y. Selenium Nanoparticles Derived from Moringa Oleifera Lam. Polysaccharides: Construction, Stability, and In Vitro Antioxidant Activity. *Foods* **2025**, *14*, 918, https://doi.org/10.3390/foods14060918.
61. Huang, Y.; Tan, J.; Wang, G.; Zhou, L. Selenium Nanoparticles for Antioxidant Activity and Selenium Enrichment in Plants. *ACS Appl. Nano Mater.* **2024**, *7*, 12881–12890, https://doi.org/10.1021/acsanm.4c01446.
62. Kokila, K.; Elavarasan, N.; Sujatha, V. Diospyros Montana Leaf Extract-Mediated Synthesis of Selenium Nanoparticles and Its Biological Applications. *New J. Chem.* **2017**, *41*, 7481–7490, https://doi.org/10.1039/C7NJ01124E.
63. Menon, S.; Agarwal, H.; Shanmugam, V.K. Catalytical Degradation of Industrial Dyes Using Biosynthesized Selenium Nanoparticles and Evaluating Its Antimicrobial Activities. *Sustain. Environ. Res.* **2021**, *31*, 2, https://doi.org/10.1186/s42834-020-00072-6.
64. Hassanien, R.; Abed-Elmageed, A.A.I.; Husein, D.Z. Eco-Friendly Approach to Synthesize Selenium Nanoparticles: Photocatalytic Degradation of Sunset Yellow Azo Dye and Anticancer Activity. *ChemistrySelect* **2019**, *4*, 9018–9026, https://doi.org/10.1002/slct.201901267.
65. Soheyli, F.; Hassani, H.; Darroudi, M. Biosynthesis of Selenium Nanoparticles Using Trigonella Foenum-Graecum L Extract and Examination of Their Photocatalytic and Cytotoxic Properties. *Int. J. Environ. Sci. Technol.* **2025**, *22*, 1017–1028, https://doi.org/10.1007/s13762-024-05853-9.

Publisher's Note & Disclaimer